RSC Advances

PAPER

View Article Online
View Journal | View Issue

Cite this: *RSC Adv.*, 2017, **7**, 18231

Factors affecting *p*-nitrophenol removal by microscale zero-valent iron coupling with weak magnetic field (WMF)†

Juanshan Du, Di Che, Xiaofan Li, Wanqian Guo* and Nanqi Ren*

The effect of WMF on the kinetics of *p*-nitrophenol (PNP) removal by six commercial zero-valent iron (ZVI) samples from different origins were studied at pH 4.0. The pseudo-first-order rate constant (k_{obs}) of PNP removal by ZVI with WMF were 2.9–5.4-fold greater than those without WMF. The strong correlation between the specific reaction rate constants (k_{SA}) of PNP removal by various ZVI samples and the specific rate constant of Fe(II) release ($k_{Fe(II)\ release\ SA}$) during these processes indicated that enhancement of PNP removal by ZVI in the presence of WMF was mainly ascribed to the improved Fe^0 corrosion and Fe(II) generation. Effects of pH value (4.0–7.0), ZVI loading (100–1000 mg L^{-1}), PNP concentration (5–100 μM), magnetization time (1–120 min), and various anions (at 1–50 μM concentration) on PNP removal by ZVI with and without the presence of WMF was investigated. The presence of WMF significantly accelerated PNP removal at pH 4.0–7.0, especially at neutral pH values. The k_{SA} and $k_{Fe(II)\ release\ SA}$ linearly increased with increasing ZVI loading, and the enhancement factor is stable with increasing ZVI loading. PNP concentration exhibited a very slight effect on PNP removal with and without WMF. The k_{obs} of PNP removal increased with increased magnetization time and trended to be consistent for more than 5 min of magnetization by WMF. WMF exhibited a positive effect on PNP removal in the presence of sulfate, chlorate, and nitrate. Although perchlorate could inhibit PNP removal by ZVI, WMF decreased the negative effect of perchlorate on PNP removal by ZVI. Furthermore, the possible degradation pathway of PNP degradation by ZVI was proposed according to the detected intermediates.

Received 17th February 2017
Accepted 13th March 2017

DOI: 10.1039/c7ra02002c

rsc.li/rsc-advances

Introduction

The increasing occurrence of organic chemical pollution in the aquatic environment, reported by various studies, has also raised widespread concern over its adverse effects on aquatic ecology and risks to human health.[1] Nitrophenols, an important category of industrial raw materials, have been widely used as precursors or intermediates in the production of pesticides, pharmaceuticals, synthetic dyes, explosives, and rubber chemicals.[2–4] Three nitrophenols (2-nitrophenol, 4-nitrophenol, and 2,4-dinitrophenol) have been listed as priority pollutants in water by the U.S. Environmental Protection Agency (EPA) since 1979 for their toxicity, biorefractory effects, potential carcinogenicity, and mutagenicity.[5] Usually, nitrophenols have possessed strong resistance to chemical and biological oxidation for the electron-withdrawing nitro group on the benzene ring; nevertheless, nitrophenols are reduced to limited products of nitrosophenols or aminophenols by anaerobic biological treatments, which still exhibit environmental risks.[6] As a priority nitrophenol, 4-nitrophenol (*p*-nitrophenol or PNP) is easily released to water[7] and soil[2] during its production and application due to its high stability and solubility, and it has received wide attention for its hazardous effects on the blood, liver and central nervous system of human beings.[8] Thereby, it is essential to control the concentration of PNP in aquatic environments by developing efficient technologies.

Many studies have employed that various techniques, such as advance oxidation process (AOPs),[9] adsorption,[10] and reduction,[11] to control PNP in water and wastewater treatment processes. Zero-valent iron (ZVI or Fe^0), as a green reductive reagent, has shown the combined effects of reduction, adsorption, co-precipitation and oxidation on contaminant degradation in water. ZVI has been widely applied to remove various pollutants such as azo dye, nitroaromatics, halogenated organic compounds, nitrate, perchlorate, and many heavy metals since 1996.[12–15] Generally, the contaminant degradative rate of ZVI is dependent on the surface area and abundant reactive surface sites of ZVI samples. Thus, nanoscale ZVI (nZVI) has been proposed to replace the microscale ZVI to improve the performance of Fe^0.[16] However, the synthesis of nZVI has been

State Key Laboratory of Urban Water Resource and Environment, Harbin Institute of Technology, Harbin 150090, PR China. E-mail: guowanqian@126.com; rnq@hit.edu.cn; Fax: +86-451-86283008; Tel: +86-451-86283008

† Electronic supplementary information (ESI) available. See DOI: 10.1039/c7ra02002c

considered too expensive for the costly reagents and complex processes.[17] Besides, nZVI surface passivation should be carried out before handling due to its high reactivity, and the potential toxicity of nZVI and derivatives has raised much concern.[18] Recently, Guan *et al.*[19,20] have done many comprehensive studies on weak magnetic field (WMF) enhancing the removal of several heavy metals by microscale ZVI. The application of an inhomogeneous weak magnetic field (WMF) (B_{max} < 20 mT) could significantly enhance Se(IV) removal by both pristine ZVI and aged ZVI[19,20] and greatly improve As(V) and As(III) removal by Fe^0 at pH_{ini} 3.0–9.0.[21] The accelerated Se(IV), As(III) and As(V) removal by Fe^0 was mainly ascribed to the improved Fe^0 corrosion and Fe(II) generation. Besides, premagnetized multiple ZVI samples also enhanced the degradative rates of various heavy metals, and the strong correlations between the Fe(II) generation rates of various pristine ZVI/premagnetized ZVI samples and the removal rate constants of a specific contaminant by these ZVI samples was also observed.[22] Although very few studies have been conducted to investigate heavy metals removal by microscale ZVI in the presence of WMF, the limited information revealed the efficient removal of organics in a Fe^0/H_2O process.

Therefore, in the present study, PNP was chosen as target contaminant to investigate the effect of selected factors on PNP degradation by Fe^0. The objectives of this study are to (1) compare the removal rates of PNP by multiple ZVI samples with or without WMF, (2) assess the effects of pH, initial ZVI loadings, PNP concentration, and magnetization time on PNP degradation by Fe^0 with or without WMF, (3) determine the effects of several background anions on PNP degradation by Fe^0 with or without WMF, and (4) clarify PNP degradation pathways by Fe^0.

Experimental

Materials

PNP of 99% purity was purchased from Sigma-Aldrich Co. LLC. (St. Louis, MO, USA). Six commercial ZVI (≥99% pure) samples including granular ZVI (about 400 mesh) and microscale ZVI were supplied by Sinopharm Chemicals Reagent Co., Ltd. (Shanghai, China), Shanghai Yunfu Nanotechnology Co., Ltd. (Shanghai, China), Shanghai Haotian Nanotechnology Co., Ltd. (Shanghai, China), and Sigma-Aldrich Co. LLC. (St. Louis, MO, USA). All chemicals were used without further purification, and solutions were prepared with deionized (DI) water.

Batch experiments

The batch experiments were conducted in a plexiglass reactor (14 cm height × 10 cm diameter) open to the air at 20 ± 1.0 °C, and 0.5 L solution containing PNP was completely mixed by digital display electric blender at 500 rpm. The nonuniform WMF was generated by positioning two thin cylindrical neodymium–iron–boron permanent magnets at the bottom of the reactor. To maintain pH of the solutions constant (±0.1), buffers of 100 mM sodium acetate, 100 mM 2-(*N*-morpholino) ethanesulfonic acid (MES), and 40 mM piperazine-*N*,*N*′-bis(ethanesulfonic acid) (PIPES) were employed for pH 4.0–5.0, 6.0, and 7.0, respectively. The negligible interferences from MES and PIPES buffers forming non-complexes with Fe(II) or Fe(III) in these reactions have been extensively discussed.[23] Experiments were initiated after addition of ZVI into the reactor. For the kinetic study, at fixed time intervals, a 10 mL sample was rapidly transferred into a 25 mL beaker which was immediately quenched with 100 μL of methanol, filtered with 0.22 μm membrane and collected into sample vials quickly.

Chemical analysis

A high-performance FE20-FiveEasy pH meter with a saturated KCl solution as electrolyte produced by Mettler-Toledo (Switzerland) was employed to measure solution pH, and daily calibration with standard buffers (pH 4.00, 6.86 and 9.18) was necessary to ensure its accuracy.

The BET surface areas of all ZVI samples were determined by Quantachrome Instruments Quadrasorb SI-MP-21 (Boynton Beach, FL, USA) and are listed in Table S1.†

PNP was analysed by a Waters ACQUITY ultra-performance liquid chromatography (UPLC) system including a binary solvent manager (BSM) and a sample manager (SM) with a UV detector (TUV) (Milford, MA, USA). Separation was accomplished with an UPLC BEH C18 column (2.1 × 50 mm, 1.7 μm; Waters) at 35 ± 1.0 °C with a mobile phase of two effluents (effluent A: 30% acetonitrile with 0.1% formic acid; effluent B: 70% H_2O with 0.1% formic acid) at a flow rate of 0.1 mL min^{-1}. Concentrations of PNP were determined by comparing the peak area at 318 nm with that of standards. The intermediate products of PNP degradation were separated by the Agilent 1290 Infinity interfaced with a triple quadrupole mass detector (6400) (UHPLC-MS) (Santa Clara CA, United States). Mass spectral analysis was conducted in positive and negative mode electrospray ionization ((+)ESI and (−)ESI) over a mass range of 50–300 *m*/*z*. The fragment used was 110 V conducted in auto full scan mode (MS). Details of the UHPLC method are similar to the conditions for SMX quantification mentioned above.

Results and discussion

Influence of WMF on the kinetics of PNP removal by multiple ZVI samples

The raw time courses of aquatic PNP degradation by various ZVI samples (*i.e.*, Guoyao, Sigma, HT1, YF1, HT2, and YF2) with and without WMF are presented in Fig. S1,† and all kinetic data are used in subsequent kinetic analyses. Obviously, WMF exhibited various degrees of enhancement on the reactivity of multiple ZVI samples toward PNP removal and promoted the corresponding Fe(II) release during the process of PNP removal by ZVI (as shown in Fig. S2†). A pseudo-first-order kinetic model,[24] as shown in eqn (1), was employed to quantitatively describe the influence of WMF on the reactivity of ZVI. Simulative results of PNP elimination are illustrated by the solid or dashed lines in Fig. S1,† and the calculated rate constants of PNP removal by ZVI with and without WMF are summarized in Fig. 1.

$$-\frac{d[PNP]}{dt} = k_{obs}[PNP] = k_{SA}\rho_a[PNP] \quad (1)$$

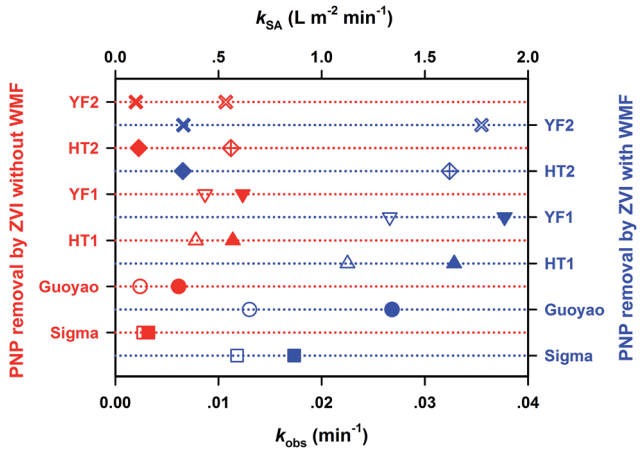

Fig. 1 Pseudo-first-order rate constants (k_{obs}, min^{-1}, empty symbols) and normalized specific reaction rate constants (k_{SA}, L m^{-2} min^{-1}, filled symbols) of PNP removal by ZVI without (left ordinate) and with (right ordinate) WMF. Reaction conditions: [Fe^0] = 0.10 g L^{-1}, [PNP] = 10 μM, [NaAc-HAc] = 0.10 M (pH 4.0), rpm = 500, T = 20 ± 1 °C.

where k_{obs} is the pseudo-first-order rate constant (min^{-1}) of PNP removal by ZVI, k_{SA} is the normalized specific reaction rate constant (L m^{-2} min^{-1}) of PNP removal, and ρ_a is the surface area concentration of ZVI (m^2 L^{-1} of solution, calculated from Table S1†). The rate constants provided by Fig. 1 reveal that different k_{obs} values of PNP removal by ZVI **samples vary by origins. Moreover, WMF significantly increases the rate constants of PNP removal by all applied ZVI samples. Although the increase is not uniform for different ZVI samples, the mean value of rate constants was increased appreciably from 0.0073 to 0.0236 min^{-1} after the WMF radiation. However, the value of k_{obs} cannot really exhibit the reactivity of ZVI toward a specific contaminant, even under the same experimental conditions for ZVI, from different sources with different iron surface area concentrations. Thus, the k_{obs} data should be normalized to the specific rate constants (k_{SA}) by eqn (1), and the obtained k_{SA} values are summarized in Fig. 1. The mean value of k_{SA} was increased appreciably from 0.311 to 1.066 L m^{-2} min^{-1} after the radiation of WMF.

Meanwhile, the Fe(II) concentration increased almost linearly with time with the degradation of PNP, and a zero-order reaction kinetic model[25] (eqn (2)) was employed to quantitatively describe the influence of WMF on the release of Fe(II). The simulative kinetics of Fe(II) release from ZVI with and without WMF at pH 4.0 buffered with NaAc-HAc, open to the air, are shown in Fig. S2,† and the calculated Fe(II) release rate constants ($k_{Fe(II)\ obs}$) and normalized Fe(II) release rate constants ($k_{Fe(II)\ release\ SA}$) are summarized in Fig. S3.† Obviously, WMF significantly increased the normalized Fe(II) release rate, which indicates that ZVI corrosion was enhanced after the addition of WMF.

$$\frac{d[Fe(II)]}{dt} = k_{Fe(II)\ obs} = k_{Fe(II)\ release\ SA}\rho_a \quad (2)$$

where $k_{Fe(II)\ obs}$ represents the zero-order rate constant (mg L^{-1} min^{-1}) of Fe(II) release, and $k_{Fe(II)\ release\ SA}$ is the normalized Fe(II) release rate constant (mg m^{-2} min^{-1}).

Generally, it is expected that the rate constants of PNP removal by different types of ZVI under identical reaction conditions are positively related to the Fe(II) release of these ZVI samples. The investigation of Li *et al.*[22] revealed the Pearson correlation of the specific rate constants for heavy metal removal with the specific rate constant of Fe(II) generation. Hence, the Pearson correlations of the rate constants (lg k_{SA}) for PNP removal by six ZVI samples with the release rate constant (lg $k_{Fe(II)\ release\ SA}$) of these ZVI samples in the presence and absence of WMF are demonstrated in Fig. 2.

The correlation coefficients of lg k_{SA} for PNP removal by six types of ZVI with lg $k_{Fe(II)\ release\ SA}$ in the presence and absence of WMF were 0.96 and 0.80, respectively. The good correlation coefficients indicated that the degradation of PNP was accompanied by a release of Fe(II). Thus, the results of the Pearson correlations can be employed for the removal rate constant of the contaminant by a ZVI sample with WMF and without WMF from its Fe(II) release rate.

Effects of treatment factors tested

Effect of pH. The effect of WMF on PNP removal by ZVI (as shown in Fig. 3) and the variation of Fe(II) release (as shown in Fig. S4†) in this process are investigated in the pH range of 4.0–7.0. In the absence of WMF, the kinetics of PNP removal by ZVI exhibited a short lag phase of about 5 min before the initiation of a rapid removal period at pH 4.0 and 5.0. The lag period of PNP removal by ZVI increased to 300 min as pH increased to 6.0. The increasing lag period with pH increase was ascribed to the formation of secondary reductants before the reduction of contaminants and the removal of the iron oxide layer.[25] When pH increased to 7.0, PNP was hardly degraded by ZVI during 480 min of mixing, which indicated that the reactivity of ZVI was significantly weakened at neutral pH. The release of Fe(II) also

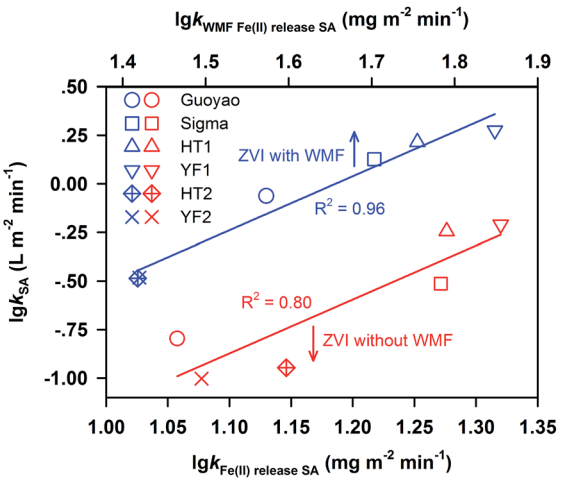

Fig. 2 Pearson correlation of the specific rate constants (lg k_{SA}, L m^{-2} min^{-1}) of PNP removal by ZVI with the release rate constant (lg $k_{Fe(II)\ release\ SA}$ or lg $k_{WMF\ Fe(II)\ release\ SA}$, mg m^{-2} min^{-1}) of these ZVI samples in the presence and absence of WMF. Reaction conditions: [Fe^0] = 0.10 g L^{-1}, [PNP] = 10 μM, [NaAc-HAc] = 0.10 M (pH 4.0), rpm = 500, T = 20 ± 1 °C.

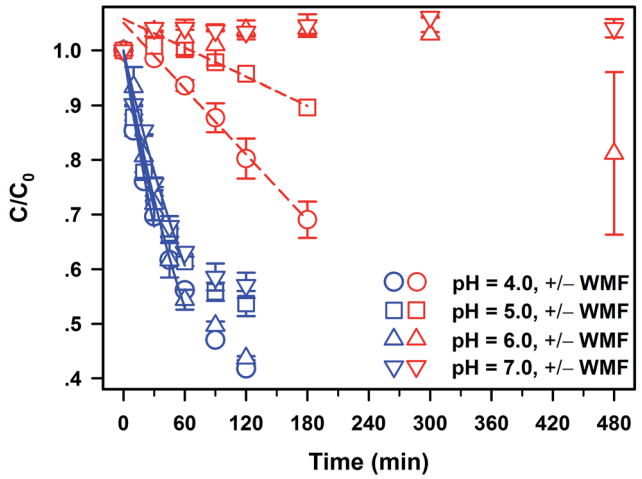

Fig. 3 Effects of pH on PNP removal by ZVI with and without WMF. Reaction conditions: $[PNP]_0 = 10$ μM, $[ZVI_{Guoyao}]_0 = 100$ mg L^{-1}, rpm = 500, and $T = 20 \pm 1$ °C. Solid and dashed lines represent simulative results.

proved that the corrosion of ZVI was dependent on pH. As mentioned above, the presence of WMF accelerated the removal of PNP at pH 4.0, which was in accordance with the release of Fe(II). The positive effect of WMF on PNP removal and Fe(II) release was also observed at pH 5.0. More importantly, the application of WMF significantly enhanced the removal of PNP at pH 6.0 and 7.0. The removal rate of PNP (at 120 min) by ZVI reached 56% and 43% at pH 6.0 and 7.0, respectively. Generally, the degradation of PNP was ascribed to the reduction of ZVI and oxidation of $^{\bullet}OH$ at pH 4.0 and 5.0, and the reduction of ZVI and oxidation of the ferryl ion (Fe(IV)) generated by Fe(II)/O_2 at pH 6.0 and 7.0.[13,23] The efficiency of the reduction by ZVI and oxidation of $^{\bullet}OH$ or Fe(IV) was based on the corrosion of ZVI and generation of Fe(II). As shown in Fig. S4,† the application of WMF-enhanced iron corrosion of ZVI at pH 4.0–7.0 and the release rate of Fe(II) showed very little difference with increasing pH from 4.0 to 7.0. The irregular variation of PNP removal rate by ZVI with WMF at various pH levels indicated that the contribution of oxidative species generated by ZVI and the reduction by ZVI was different with pH increasing from 4.0 to 7.0.

Effect of initial ZVI loading

The effect of initial ZVI loading from 100 to 500 mg L^{-1} on PNP removal by ZVI with and without WMF open to the air, and the variation of Fe(II) release kinetics in this process, are shown in Fig. S5.† In addition, simulative results of PNP elimination by eqn (1) and of Fe(II) release by eqn (2) are illustrated by the solid or dashed lines in Fig. S5.† In the absence of WMF, the lag phase was shortened with increased ZVI loading. Kinetics of Fe(II) release also showed a similar variation of the short lag period, which is consistent with the results of PNP removal. Thus, increasing ZVI loading can shorten the lag period and accelerate the removal of contaminants. To quantitatively describe the influence of ZVI loading on PNP removal by ZVI and Fe(II) release, linear correlations of k_{obs} of PNP removal and $k_{Fe(II)\ obs}$ of Fe(II) release in the presence and absence of WMF with ZVI loading are shown in Fig. 4. The good correlation between k_{obs} (or $k_{Fe(II)\ obs}$) and ZVI loading mainly was ascribed to the linear increase of ZVI surface area, which contributed to PNP removal and Fe(II) release. The application of WMF-enhanced PNP removal by ZVI eliminated the lag period. The enhancing factor of WMF, as the ratio of the slope in linear regression results, is stable with increasing ZVI loading, which indicates that WMF does not weaken the enhancement on ZVI reactivity with increasing ZVI loading.

Effect of initial PNP concentration

Fig. S6† illustrates the effect of initial PNP concentration (C_0) ranging from 5 to 100 μM on PNP removal by ZVI and Fe(II) release during these processes. The initial PNP concentration showed slight influence on PNP removal and Fe(II) release. The addition of WMF also accelerated PNP removal and enhanced Fe(II) release, and increasing PNP concentration inhibited the enhancing effect of WMF. As shown in Fig. 5, degradative rates ($k_{obs} \times C_0$) of PNP and Fe(II) release rates ($k_{Fe(II)\ obs} \times C_0$) linearly increase with increasing initial PNP concentrations in the presence and absence of WMF. This behaviour was well fitted by first-order kinetics (eqn (3)) similar to the initial phase of the modified Langmuir–Hinshelwood equation, which has been applied in contaminant removal by ZVI.[26] Thus, WMF does not change the kinetics of PNP removal by ZVI and Fe(II) release but improves the identical reactivity of ZVI (V_m) towards PNP.

$$-\frac{d[PNP]}{dt} = \frac{V_m[PNP]}{K_{1/2} + [PNP]} = \frac{V_m}{K_{1/2}}[PNP] \quad (\text{when } K_{1/2} \gg [PNP]) \tag{3}$$

where V_m represents the maximum reaction rate (μM min^{-1}) and $K_{1/2}$ is a constant reflecting the affinity of the iron surface for PNP.

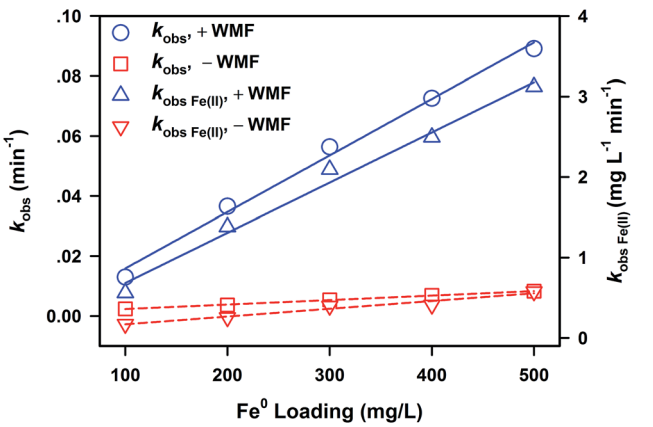

Fig. 4 Linear correlations of k_{obs} of PNP removal by ZVI_{Guoyao} and $k_{Fe(II)\ obs}$ of Fe(II) release in the presence and absence of WMF with ZVI loading. Reaction conditions: [PNP] = 10 μM, [NaAc-HAc] = 0.10 M (pH 4.0), rpm = 500, $T = 20 \pm 1$ °C. Solid and dashed lines represent simulative results.

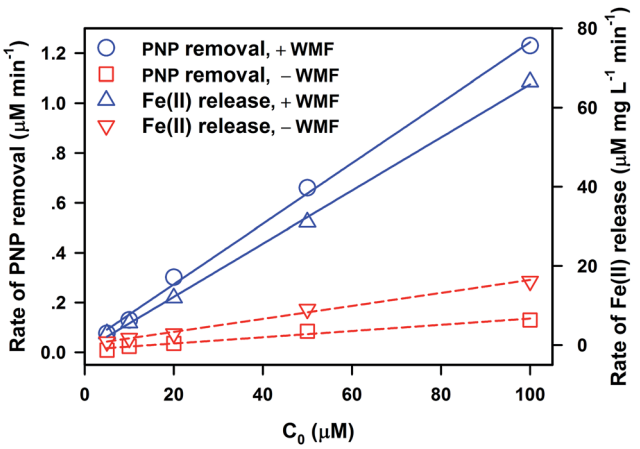

Fig. 5 Effect of initial PNP concentration on degradative rates ($k_{obs} \times C_0$) of PNP removal by ZVI and Fe(II) release rates ($k_{Fe(II)\ obs} \times C_0$) during these processes. Reaction conditions: $[ZVI_{Guoyao}]_0$ = 100 mg L^{-1}, [NaAc-HAc] = 0.10 M (pH 4.0), rpm = 500, $T = 20 \pm 1$ °C. Solid and dashed lines represent simulative results.

Effect of magnetization time

WMF-enhanced PNP removal by ZVI, by applying a weak magnetic field in a large treatment unit during the reaction, should overcome the increasing cost of operating magnetic field devices. Hence, Guan *et al.*[19,22] developed ZVI premagnetization before the reaction to enhance the reactivity of ZVI toward various contaminants. However, the reactivity of premagnetized ZVI was not stable and decreased with time before the reaction. In this study, the *in situ* variation of ZVI reactivity towards PNP with magnetization time was studied. Fig. 6 shows the effect of magnetization time on PNP removal kinetics by ZVI at pH 4.0, and measured reaction time courses of Fe(II) release during these processes are also summarised in Fig. S7.† The enhanced reactivity of ZVI towards PNP increased with increasing magnetization time from 1 to 120 min. The effect of magnetization time on PNP removal rate and Fe(II) release rate could be ignored in the presence of WMF for more than 5 min. The high efficiency of PNP removal by ZVI with WMF in a short magnetization time was interpreted as the magnetic memory of ZVI, maintaining ZVI reactivity during the reaction processes.[22] Shortened magnetization time may give engineering implications on the application of WMF on ZVI.

Effects of common dissolved anions on WMF-enhanced PNP removal by ZVI

Batch kinetics were conducted to study PNP removal by ZVI with and without WMF in the presence of various anions including Cl^-, SO_4^{2-}, NO_3^-, and ClO_4^-. The raw time courses of PNP removal by ZVI are shown in Fig. S8.† The measured reaction time courses of PNP removal during these processes are modelled by eqn (1), and corresponding rate constants are summarized in Fig. 7. Sulfate and chloride anions always exhibited positive effects on PNP removal regardless of the presence or absence of WMF. Sulfate could remove iron oxides and hydroxides from the iron surface, which increased the reactive sites of ZVI reacted with PNP. Although Sugimoto and Wang[27] reported that a high sulfate concentration beyond 50 mg L^{-1} might inhibit the reactivity of ZVI in the precipitation of acicular α-FeOOH and precipitation of basic ferric sulfate iron surface, sulfate always enhanced PNP removal, even at 50 mM, in this study. Chloride could passivate oxides on the iron surface and form strong complexes with ZVI.[28] Thus, oxides on reactive sites were cleaned by chloride, and PNP removal was accelerated. However, nitrate anions always exhibited diverse effects on PNP removal in the presence and absence of WMF. Since nitrate was reduced by ZVI, reactivity of ZVI towards PNP was decreased for the competition of nitrate.[28] Curiously, it was found in this study that the presence of WMF and nitrate did not decrease PNP removal rate or even exhibit a slightly positive effect on PNP removal. Perchlorate anions inhibited PNP removal by ZVI because perchlorate could occupy some

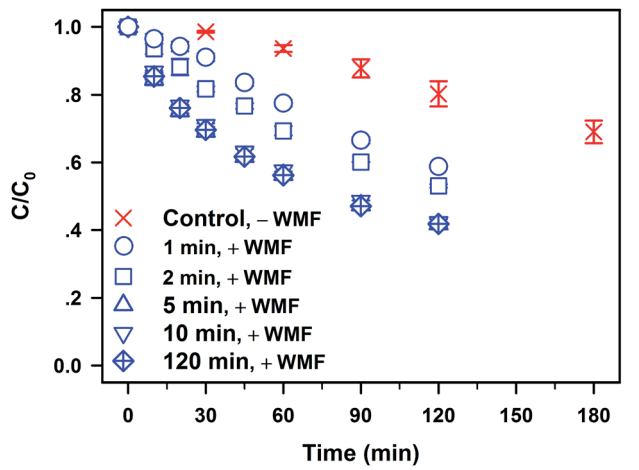

Fig. 6 Effect of magnetization time on PNP removal kinetics by ZVI. Reaction conditions: $[ZVI_{Guoyao}]_0$ = 100 mg L^{-1}, [PNP] = 10 μM, [NaAc-HAc] = 0.10 M (pH 4.0), rpm = 500, $T = 20 \pm 1$ °C.

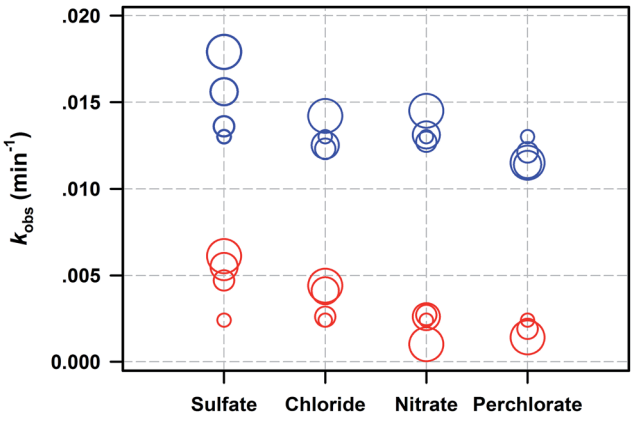

Fig. 7 Summary of k_{obs} for PNP removal by ZVI *vs.* dissolved anions. The circle size represents the concentration of anions. The values of k_{obs} for all these data are given in Table S2.† Reaction conditions: $[ZVI_{Guoyao}]_0$ = 100 mg L^{-1}, [PNP] = 10 μM, [NaAc-HAc] = 0.10 M (pH 4.0), rpm = 500, $T = 20 \pm 1$ °C.

reactivity sites of ZVI with PNP, which decreased PNP removal rate. In addition, WMF could not reverse the negative effect of perchlorate on PNP removal by ZVI. Overall, in the presence of various anions, the application of WMF was considered as a superior strategy for contaminant removal by ZVI.

Possible degradation pathways of PNP by ZVI with and without WMF

Many studies have identified the degradation intermediates of PNP by various processes. The species of reaction intermediates and degradation pathways of PNP removal, even in different AOPs identified by GC-MS, LC-MS, and HPLC, were different. In this study, UHPLC-MS was employed to detect the reaction intermediates of PNP by ZVI at pH 4.0, based on which the PNP degradation pathways were proposed.

It was found that WMF had no influence on the varieties of detected intermediates, which indicated that WMF enhanced PNP removal without changing the PNP degradation pathways. Five reaction intermediates were detected in the process of PNP removal, which are summarized in Table S3.† Based on the detected intermediates specified in this study, two proposed transformation pathways (I and II) by ZVI leading to PNP degradation are presented in Fig. 8. In pathway I, reduction of PNP formed P1 (*p*-nitrosophenol), and P1 was reduced to P2 (*p*-aminophenol). This degradation pathway is considered as the classical reductive process also observed in PNP reduction by nZVI.[3]

It has been reported that the reaction of ZVI or nZVI and oxygen could produce reactive oxidants capable of oxidizing organics.[29] Oxidation under acidic conditions is attributable to the generation of H_2O_2 during ZVI oxidation, which then reacts with Fe(II) *via* the Fenton reaction to produce ˙OH. Thus, the second main reaction pathway (II) was PNP oxidation by ˙OH. It is well known that the reaction of ˙OH with aromatic groups occurs *via* electrophilic addition.[9,23] In pathway II, electrophilic addition on the aromatic ring by ˙OH formed P3 (*p*-nitrocatechol), which could also be frequently detected in AOPs processes, as demonstrated in Fig. 8. On the subsequent ˙OH attack, the PNP was converted into P4 (*p*-nitropyrogallol) or P5 (*o*-nitrobenzoquinone). The further oxidation of P4 and P5 by ˙OH resulted in the aromatic ring opening, formation of aliphatic acids, and eventual generation of mineralization products.

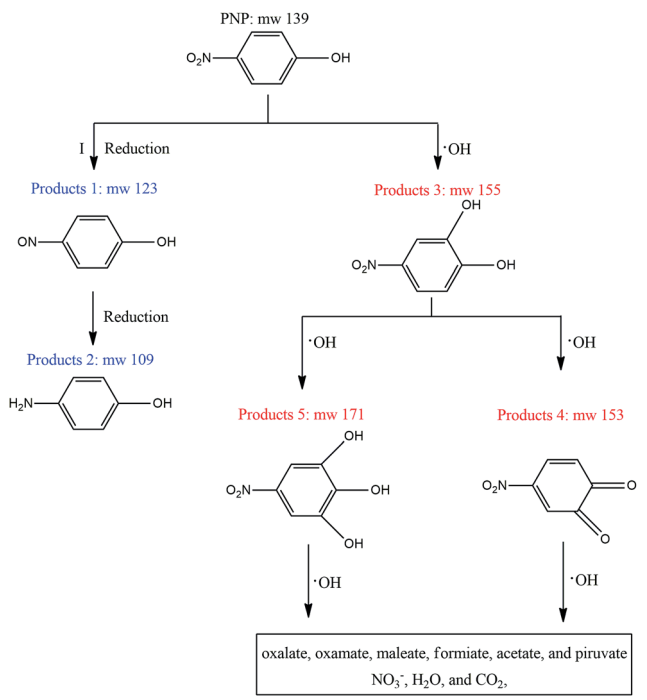

Fig. 8 Possible degradation pathways of PNP by ZVI.

Conclusions

The application of WMF induced a significant enhancement in PNP removal rates by various ZVI samples from different origins at pH 4.0. The strong correlation between the specific reaction rate constants (k_{SA}) of PNP removal by various ZVI samples and the specific rate constants of Fe(II) release ($k_{Fe(II)\ release\ SA}$) during these processes indicated that the reactivity of different ZVI samples depended on the release of Fe(II) and that the presence of WMF promoted iron corrosion and Fe(II) generation. WMF significantly accelerated PNP removal at pH 4.0–7.0, which was ascribed to the enhanced corrosion of ZVI in the presence of WMF. k_{SA} and $k_{Fe(II)\ release\ SA}$, in the presence or absence of WMF, linearly increased with increasing ZVI loading, which suggested that the enhancing factor of WMF was independent of ZVI loading. Furthermore, PNP concentration exhibited very slight effect on PNP removal with and without WMF. PNP removal rate by ZVI did not decrease after 5 min of magnetization by WMF compared with 120 min, which was ascribed to the magnetic memory of ZVI. In addition, the short magnetization time by WMF might give an important implication on the economy and feasibility of engineering application. Effects of sulfate, chlorate, nitrate, and perchlorate anions at various concentrations on WMF-enhanced PNP removal by ZVI were investigated. WMF exhibited a positive effect on PNP removal in the presence of sulfate, chlorate, and nitrate. Although perchlorate could inhibit PNP removal by ZVI, WMF decreased the negative effect of perchlorate on PNP removal by ZVI. Furthermore, degradation pathways of PNP were proposed according to the intermediates determined by UHPLC-MS, and WMF enhanced PNP removal but did not change the PNP degradation pathways.

Acknowledgements

This work was financially supported by the National Natural Science Foundation of China (51678188) and the State Key Laboratory of Urban Water Resource and Environment (2015TS06).

References

1 J. S. Du, B. Sun, J. Zhang and X. H. Guan, *Environ. Sci. Technol.*, 2012, **46**, 8860–8867.

2 T. C. Wang, N. Lu, J. Li and Y. Wu, *Environ. Sci. Technol.*, 2011, **45**, 9301–9307.
3 L. Tang, J. Tang, G. M. Zeng, G. D. Yang, X. Xie, Y. Y. Zhou, Y. Pang, Y. Fang, J. J. Wang and W. P. Xiong, *Appl. Surf. Sci.*, 2015, **333**, 220–228.
4 Z. I. Bhatti, H. Toda and K. Furukawa, *Water Res.*, 2002, **36**, 1135–1142.
5 L. Keith and W. Telliard, *Environ. Sci. Technol.*, 1979, **13**, 416–423.
6 B. Lai, Y. H. Zhang, R. Li, Y. X. Zhou and J. L. Wang, *Chem. Eng. J.*, 2014, **249**, 143–152.
7 S. P. Sun and A. T. Lemley, *J. Mol. Catal. A: Chem.*, 2011, **349**, 71–79.
8 G. Eichenbaum, M. Johnson, D. Kirkland, P. O'Neill, S. Stellar, J. Bielawne, R. DeWire, D. Areia, S. Bryant, S. Weiner, D. Desai-Krieger, P. Guzzie-Peck, D. C. Evans and A. Tonelli, *Regul. Toxicol. Pharmacol.*, 2009, **55**, 33–42.
9 X. M. Xiong, Y. K. Sun, B. Sun, W. H. Song, J. Y. Sun, N. Y. Gao, J. L. Qiao and X. H. Guan, *RSC Adv.*, 2015, **5**, 13357–13365.
10 M. H. Entezari and T. R. Bastami, *Ultrason. Sonochem.*, 2008, **15**, 428–432.
11 B. Lai, Y. H. Zhang, Z. Y. Chen, P. Yang, Y. X. Zhou and J. L. Wang, *Appl. Catal., B*, 2014, **144**, 816–830.
12 L. J. Matheson and P. G. Tratnyek, *Environ. Sci. Technol.*, 1994, **28**, 2045–2053.
13 X. H. Guan, Y. K. Sun, H. J. Qin, J. X. Li, I. M. Lo, D. He and H. R. Dong, *Water Res.*, 2015, **75**, 224–248.
14 R. W. Gillham and S. F. O'Hannesin, *Ground Water*, 1994, **32**, 958–967.
15 C. H. Xu, B. L. Zhang, L. J. Zhu, S. Lin, X. P. Sun, Z. Jiang and P. G. Tratnyek, *Environ. Sci. Technol.*, 2016, **50**, 1483–1491.
16 C. B. Wang and W. X. Zhang, *Environ. Sci. Technol.*, 1997, **31**, 2154–2156.
17 R. A. Crane and T. B. Scott, *J. Hazard. Mater.*, 2012, **211–212**, 112–125.
18 L. J. Xu and J. K. Wang, *J. Hazard. Mater.*, 2011, **186**, 256–264.
19 L. P. Liang, X. H. Guan, Z. Shi, J. L. Li, Y. N. Wu and P. G. Tratnyek, *Environ. Sci. Technol.*, 2014, **48**, 6326–6334.
20 L. P. Liang, W. Sun, X. H. Guan, Y. Y. Huang, W. Y. Choi, H. L. Bao, L. N. Li and Z. Jiang, *Water Res.*, 2014, **49**, 371–380.
21 Y. K. Sun, X. H. Guan, J. M. Wang, X. G. Meng, C. H. Xu and G. M. Zhou, *Environ. Sci. Technol.*, 2014, **48**, 6850–6858.
22 J. X. Li, H. J. Qin and X. H. Guan, *Environ. Sci. Technol.*, 2015, **49**, 14401–14408.
23 C. R. Keenan and D. L. Sedlak, *Environ. Sci. Technol.*, 2008, **42**, 1262–1267.
24 T. L. Johnson, M. M. Scherer and P. G. Tratnyek, *Environ. Sci. Technol.*, 1996, **30**, 2634–2640.
25 L. P. Liang, W. J. Yang, X. H. Guan, J. L. Li, Z. J. Xu, J. Wu, Y. Y. Huang and X. Z. Zhang, *Water Res.*, 2013, **47**, 5846–5855.
26 S. Nam and P. G. Tratnyek, *Water Res.*, 2000, **34**, 1837–1845.
27 T. Sugimoto and Y. S. Wang, *J. Colloid Interface Sci.*, 1998, **207**, 137–149.
28 W. Z. Yin, J. H. Wu, P. Li, X. D. Wang, N. W. Zhu, P. X. Wu and B. Yang, *Chem. Eng. J.*, 2012, **184**, 198–204.
29 S. H. Joo, A. J. Feitz and T. D. Waite, *Environ. Sci. Technol.*, 2004, **38**, 2242–2247.